COMMUNICATIONS IN NUMERICAL METHODS IN ENGINEERING
*Commun. Numer. Meth. Engng* 2009; **25**:53–63
Published online 1 February 2008 in Wiley InterScience (www.interscience.wiley.com). DOI: 10.1002/cnm.1105

# A model of incompressible isotropic hyperelastic material behavior using spline interpolations of tension–compression test data

Theodore Sussman[1] and Klaus-Jürgen Bathe[2,*,†]

[1]*ADINA R & D, Inc., Watertown, MA 02472, U.S.A.*
[2]*Massachusetts Institute of Technology, Cambridge, MA 02139, U.S.A.*

SUMMARY

We present a model of incompressible isotropic hyperelastic material behavior based on a strain energy description separable in terms of logarithmic strains and piecewise spline interpolations of uniaxial tension–compression test data. Valuable attributes are that no fitting of model constants is carried out and the model replicates even physically complicated test data very accurately for small and large strains and for tension and compression. The model is well suited for use in finite element analysis. Copyright © 2008 John Wiley & Sons, Ltd.

Received 11 September 2007; Revised 4 December 2007; Accepted 10 December 2007

KEY WORDS: material modeling; finite element analysis; incompressible materials; hyperelasticity; rubber-like materials

## 1. INTRODUCTION

Incompressible isotropic hyperelastic material behavior in finite element analysis [1] is usually described using one of the available hyperelasticity models, such as the Mooney–Rivlin, Ogden, and Arruda–Boyce models [2]. These material descriptions are based on measured physical behavior and theoretical considerations. The common characteristic of these material models is that they all involve some material constants to be determined from experiments. With experimental data given, the constants are fitted to best represent (in some sense) these test data over the complete strain range desired. It is then frequently found that a model represents test data well for certain levels of strains and combinations of strains but only very approximately for other conditions. Studies of hyperelasticity models and some of their limitations are, for example, given in References [2–9].

*Correspondence to: Klaus-Jürgen Bathe, Massachusetts Institute of Technology, Cambridge, MA 02139, U.S.A.
†E-mail: kjb@mit.edu

We present in this paper a quite different approach in which we avoid the fitting of material constants and, instead, we directly interpolate using spline functions the test data obtained in a uniaxial tension–compression test. Our model is based on the separable strain energy description of an incompressible isotropic hyperelastic material as, in essence, originally proposed by Mooney [4] and further by Carmichael–Holdaway [5] and Valanis–Landel [6]. Of course, the model also has limitations, but valuable attributes are that it is easy to employ and replicates accurately the test data used for large and small strains and for tension and compression.

Of course, data from strip biaxial tests can also be used to directly determine the separable strain energy density [6]. However, we focus on uniaxial tension–compression data because these data, along with equibiaxial tension data, are frequently more readily available.

In the following sections, we first present the theoretical background, then we present the model, and finally we give two illustrative examples.

## 2. THEORETICAL BACKGROUND

In this section, we summarize the theory used in the model, with emphasis on the relationship between the separable strain energy density and the uniaxial tension/compression curve.

### *2.1. The separable strain energy density assumption*

We start with the following assumption for the strain energy density $W$ of an incompressible material:

$$W = w(e_1) + w(e_2) + w(e_3) \tag{1}$$

where $w(e)$ is a function of the principal logarithmic strain (Hencky strain) and $e_1, e_2, e_3$ are the principal logarithmic strains [1]. The incompressibility condition $e_1 + e_2 + e_3 = 0$ is used along with Equation (1). This strain energy expression was proposed and studied in References [4–6]; also see References [7–9]. The expression has been shown to be applicable to many rubber-like materials.

Usually, the function $w$ is expressed in terms of the principal stretch, e.g. $w = w(\lambda)$, where $\lambda = \exp(e)$, and then $W = w(\lambda_1) + w(\lambda_2) + w(\lambda_3)$. However, there are some numerical advantages to expressing $w$ in terms of $e$. Of course, if $w = w(\lambda)$ is known, then $w = w(e)$ can be determined, and *vice versa*; hence, there is no theoretical disadvantage to using $w = w(e)$.

As an example of an available hyperelastic material model that can be expressed in the form of Equation (1), the Ogden material model corresponds to using

$$w(e) = \sum_n \frac{\mu_n}{\alpha_n}(\exp(\alpha_n e) - 1) \tag{2}$$

where $\mu_n$ and $\alpha_n$ are material constants.

Using Equation (1) and incompressibility, we note that the Cauchy stress $\tau_i$ corresponding to $e_i$ is found from

$$\tau_i = \frac{\partial W}{\partial e_i} + p = w'(e_i) + p \tag{3}$$

where $w'(e) \equiv dw/de$, and $p$ is the hydrostatic pressure. The value for $w'(0)$ is arbitrary because adding a constant to $w'(e)$ does not affect $W = w(e_1) + w(e_2) + w(e_3)$, under the condition of



DOI: 10.1002/cnm

incompressibility. Also, it is clear that, for a stable material, we need to have $W'' > 0$ for all $e_i$ subject to the incompressibility constraint, and this condition requires that $w''(e) > 0$ for all $e$.

### 2.2. *The uniaxial tension–compression curve and $w'(e)$*

In a uniaxial tension–compression test (Figure 1), we have $e_1 = e, e_2 = e_3 = -\frac{1}{2}e$. Hence, from Equation (3)

$$\tau(e) = w'(e) - w'(-\tfrac{1}{2}e) \tag{4}$$

Using Equation (4), $w'(e)$ can be determined from the uniaxial tension–compression curve $\tau(e)$, and we discuss this in detail below. Once $w'(e)$ has been determined, $w(e)$ is directly obtained by integration and can be used in Equation (1) to determine the strain energy density (and hence the material response) for general strain states.

We wish to point out that Equation (4) gives insight into the unreliability of determining the material description using simple tension data only. Given only simple tension data for $\tau(e)$, there are multiple $w'(e)$ that exactly correspond to $\tau(e)$, for positive $e$ only. Two such $w'(e)$ are

$$w'(e) = 0, \quad e < 0$$

$$= \tau(e), \quad e > 0$$

and

$$w'(e) = -\tau(-2e), \quad e < 0$$

$$= 0, \quad e > 0$$

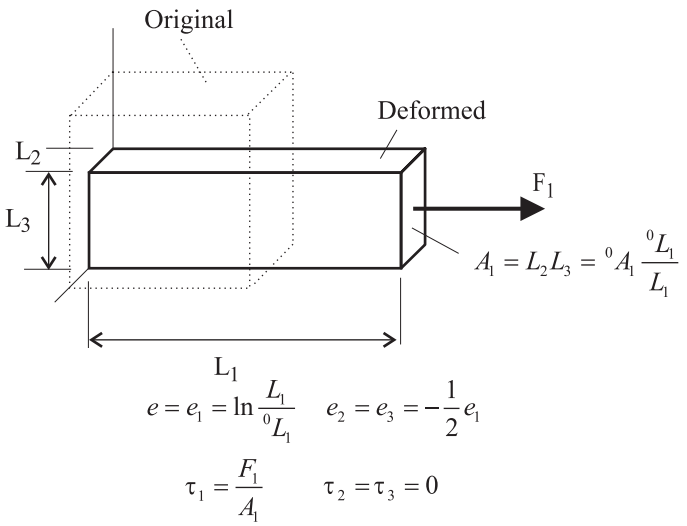


Figure 1. Uniaxial tension–compression test.



DOI: 10.1002/cnm

Substituting each of these into Equation (4) gives the original $\tau(e)$ for positive $e$, but different $\tau(e)$ for negative $e$; hence, these $w'(e)$ give different response predictions for general strain states. Hence, clearly, both tension and compression data are required.

Considering the stability of the material, it is clear that if $\tau'(e)\leqslant 0$ for some range of strains, the material is unstable. However, even if $\tau'(e)>0$ for all strains, the material might be unstable. As an example, consider a material in which

$$\begin{aligned}\tau(e) &= E_T e, \quad e>0\\ &= E_C e, \quad e<0\end{aligned}$$

where $E_T$ and $E_C$ are constants greater than zero. From Equation (4),

$$\begin{aligned}w''(e) &= \tfrac{4}{3}E_T - \tfrac{2}{3}E_C, \quad e>0\\ &= \tfrac{4}{3}E_C - \tfrac{2}{3}E_T, \quad e<0\end{aligned}$$

and $w''(e)>0$ (and hence the material is stable) only if $\frac{1}{2}E_T<E_C<2E_T$.

### *2.3. Comments concerning the determination of $w'(e)$ using curve fitting*

Given experimental data points on the uniaxial stress–strain curve (possibly using equibiaxial tension data to obtain uniaxial compression data), Equation (4) can be used in a curve-fitting approach to determine the material constants for the various available hyperelasticity models (e.g. the Ogden model). However, this curve fitting in practice may not provide a good fit to the data over the full range of strains considered. This is due, in part, to the fact that any change to the material constants affects the uniaxial stress over the entire range of strains. In addition, small changes in the experimental data points can lead to large changes in the material constants, especially when many material constants are used. The local interpolation used in the model presented below is then more effective.

## 3. THE MODEL USING SPLINES

We establish our model by first interpolating the stress–strain test data and then building an interpolation of $w'(e)$ for efficient use in finite element analysis.

### *3.1. The basic approach*

From the measured data points $(e_i, \tau_i)$, we build a piecewise spline representation of the uniaxial tension–compression stress–strain data $\tau=\tau(e)$, as shown in Figure 2. We use the test data as given, of course assuming that spurious data points have been eliminated and that roughness due to experimental procedures has been removed. This representation has the advantage that the model data passes directly through the measured data points. We use cubic splines because then $w'(e)$ and $w''(e)$ are continuous [10].

Now, to establish our model, we note that Equation (4) can be inverted to obtain

$$w'(e)=\sum_{k=0}^{\infty}\tau\left(\left(\frac{1}{4}\right)^k e\right)+\tau\left(-\frac{1}{2}\left(\frac{1}{4}\right)^k e\right) \tag{5}$$



DOI: 10.1002/cnm

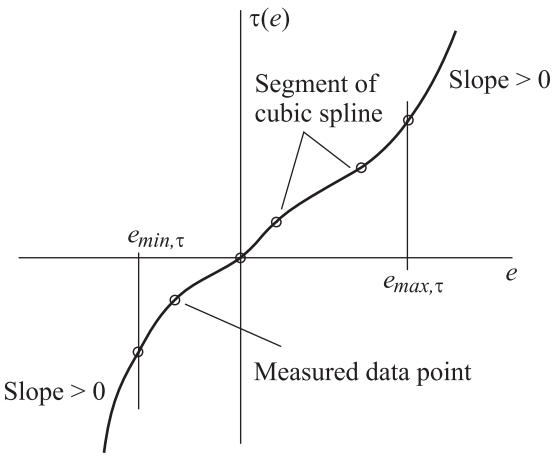


Figure 2. Uniaxial tension–compression stress–strain data represented by non-uniform piecewise splines.

provided $\tau(e) \to 0$ as $e \to 0$; see Kearsley and Zapas [7]. The $w'(e)$ given by Equation (5) satisfies Equation (4), since

$$
\begin{aligned}
&w'(e) - w'\left(-\frac{1}{2}e\right) \\
&= \left[\sum_{k=0}^{\infty} \tau\left(\left(\frac{1}{4}\right)^k e\right) + \tau\left(-\frac{1}{2}\left(\frac{1}{4}\right)^k e\right)\right] - \left[\sum_{k=0}^{\infty} \tau\left(\left(\frac{1}{4}\right)^k \left(-\frac{1}{2}e\right)\right) + \tau\left(-\frac{1}{2}\left(\frac{1}{4}\right)^k \left(-\frac{1}{2}e\right)\right)\right] \\
&= \sum_{k=0}^{\infty} \tau\left(\left(\frac{1}{4}\right)^k e\right) + \sum_{k=0}^{\infty} \tau\left(-\frac{1}{2}\left(\frac{1}{4}\right)^k e\right) - \sum_{k=0}^{\infty} \tau\left(\left(\frac{1}{4}\right)^k \left(-\frac{1}{2}e\right)\right) - \sum_{k=0}^{\infty} \tau\left(-\frac{1}{2}\left(\frac{1}{4}\right)^k \left(-\frac{1}{2}e\right)\right) \\
&= \sum_{k=0}^{\infty} \tau\left(\left(\frac{1}{4}\right)^k e\right) - \sum_{k=1}^{\infty} \tau\left(\left(\frac{1}{4}\right)^k e\right) \\
&= \tau(e)
\end{aligned}
$$

In practice, convergence is already reached to good accuracy with only a few terms in the series.

Clearly, the representation of $\tau(e)$ in Figure 2 and Equation (5) can be used to determine $w'(e)$ for any value of $e$, and the $w'(e)$ determined in this way will reproduce the piecewise representation of $\tau(e)$, and hence the original measured stress–strain data points during a uniaxial tension–compression analysis. However, the direct application of this procedure can be expensive in general finite element analysis.

### *3.2. Computational efficiency*

To obtain computational efficiency, we use the representation of $\tau(e)$ and Equation (5) to build a spline representation for $w'(e)$, as shown in Figure 3. For the representation, we use uniform



DOI: 10.1002/cnm

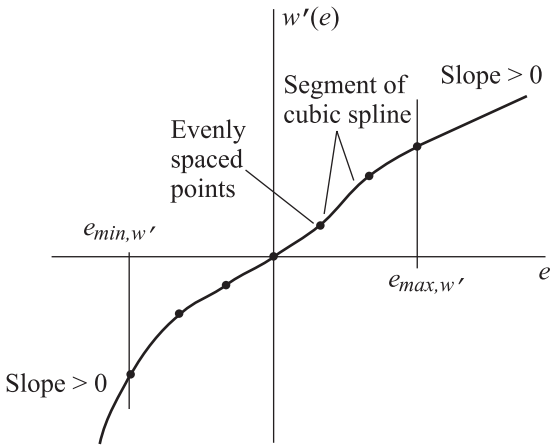


Figure 3. Representation of $w'$ by uniform piecewise splines.

cubic splines, with the same number of spline segments and the same range in tension and in compression.

This piecewise spline representation of $w'(e)$ is built as part of the preprocessing phase of finite element analysis. The computational effort required to build this representation for $w'(e)$ is negligible compared with the computational effort for the complete finite element analysis. Uniform piecewise splines are used for numerical efficiency during the finite element analysis, because then the spline segment for a given value of $e$ can be rapidly determined.

Using the representation for $w'(e)$ does not exactly reproduce the original experimental stress–strain data points during a uniaxial tension–compression analysis. However, by choosing enough spline segments in the representation for $w'(e)$, the relative interpolation error

$$r = \max_e \left| \frac{\bar{\tau}(e) - \tilde{\tau}(e)}{\tilde{\tau}(e)} \right| \tag{6}$$

where $\bar{\tau}(e)$ is the stress evaluated from the spline representation of $w'(e)$ (using Equation (4)) and $\tilde{\tau}(e)$ is the stress evaluated from the spline representation of $\tau(e)$, can be made as small as desired.

Once the representation for $w'(e)$ is obtained, the piecewise representation for $w(e)$ is easily obtained by integration. Then all quantities required in the finite element method (e.g. second Piola–Kirchhoff stresses, constitutive tensors, etc.) are directly obtained by differentiation [1].

## 4. ILLUSTRATIVE EXAMPLES

We give in this section two illustrative examples of the model and compare the results obtained with typical results given by the Ogden model. The examples are chosen, with assumed test data, merely to illustrate the capabilities of the model. Hence, we do not endeavor to fit any particular experimental data, but we use some data that are difficult to fit with the Ogden model, and we give insight into why this is so. Other material models could of course be used, but clearly models with only a few adjustable parameters cannot fit the assumed data.



DOI: 10.1002/cnm

*4.1. Neo-Hookean stress–strain test data perturbed by a bump*

Assume that the test data are given by the following function, in the strain range $-2 \leqslant e \leqslant 2$:

$$\tau(e) = \tau_{nh}(e) + \tau_p(e) \tag{7}$$

where

$$\tau_{nh}(e) = \exp(2e) - \exp(-e) \tag{8}$$

$$\tau_p(e) = \tfrac{1}{2}(1 - \cos(2\pi e)), \quad 0 \leqslant e \leqslant 1$$

$$= 0, \text{ other values of } e \tag{9}$$

These data, along with various curve fits, are shown in Figure 4. Equation (8) is the uniaxial tension–compression function for the neo-Hookean material model, with small-strain Young's modulus = 3. Equation (9) describes a small perturbation to the data, which introduces a small bump in the stress–strain curve.

The Ogden material model with only one term $\mu_1 = 1, \alpha_1 = 2$ gives a reasonable fit to the data, as must be expected since, with this choice of constants, the uniaxial tension curve for the Ogden

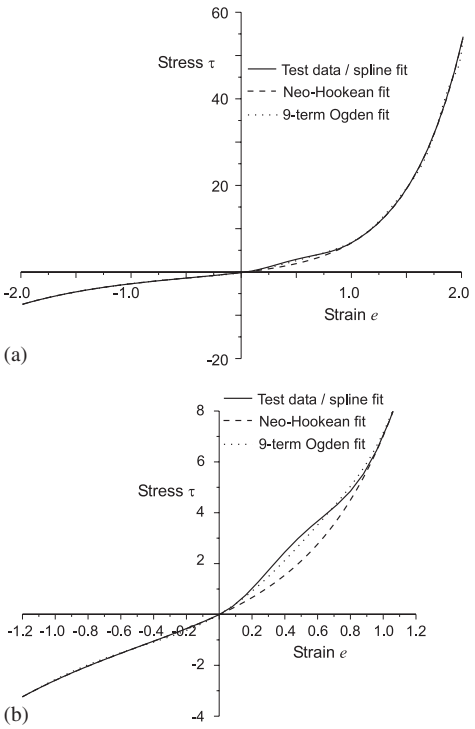


Figure 4. Assumed test data and curve fits: (a) full range of strains and (b) enlargement near the origin.



DOI: 10.1002/cnm

model reduces to Equation (8). However, this fit does not model the bump in the stress–strain curve. Increasing the number of terms in the Ogden material model to 9 allows a closer fit, but the constants are quite unrealistic; see Table I. The curve fit is seen to result from a cancellation of

Table I. Constants used for 9-term Ogden fit, for example in Section 4.1.

| $n$ | $\mu_n$ | $\alpha_n$ | $\mu_n\alpha_n$ |
|---|---|---|---|
| 1 | 16.507 | 1.0 | 16.507 |
| 2 | −49.608 | 2.0 | −99.216 |
| 3 | 66.561 | 3.0 | 199.683 |
| 4 | −45.813 | 4.0 | −183.252 |
| 5 | 18.120 | 5.0 | 90.600 |
| 6 | −4.262 | 6.0 | −25.572 |
| 7 | 0.588 | 7.0 | 4.116 |
| 8 | −0.044 | 8.0 | −0.352 |
| 9 | 0.001 | 9.0 | 0.009 |

The small-strain Young's modulus $E=\frac{3}{2}\sum\mu_n\alpha_n=3.785$.

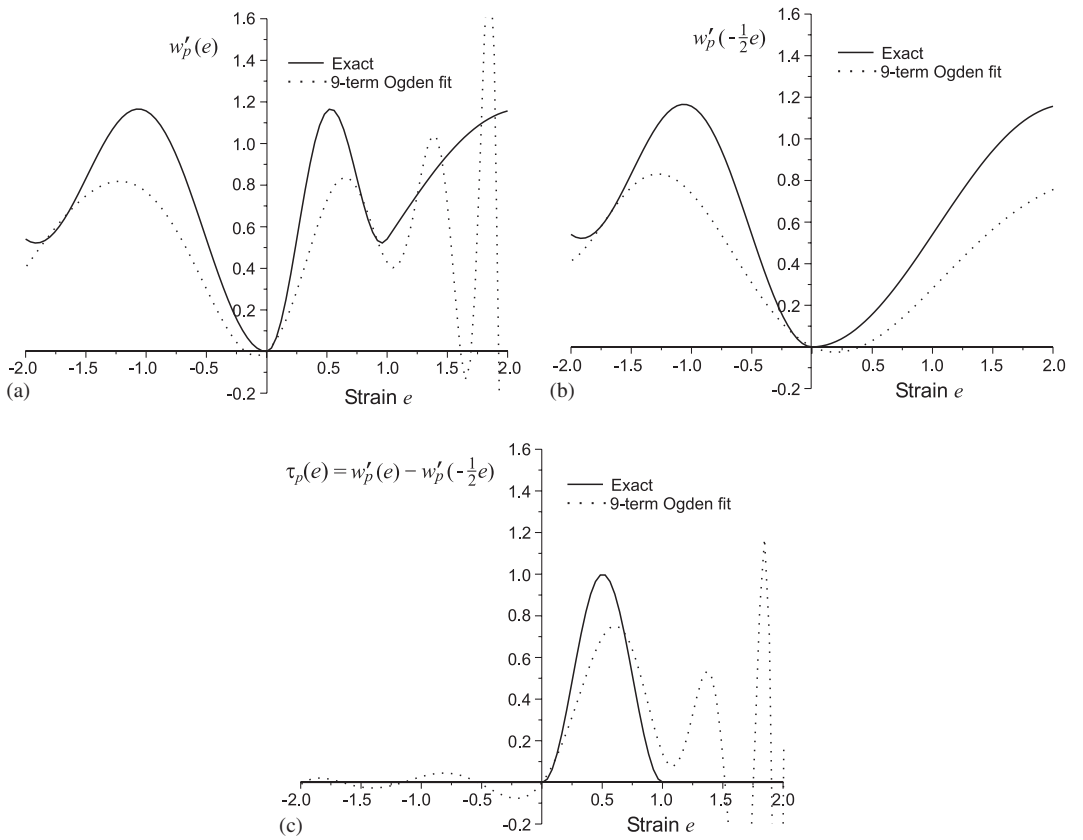


Figure 5. Comparison of exact and 9-term Ogden fits for $\tau_p$: (a) $w_p'(e)$; (b) $w_p'(-1/2e)$; and (c) $w_p'(e)-w_p'(-1/2e)=\tau_p(e)$.



DOI: 10.1002/cnm

terms of opposite signs. Other fits of constants are of course possible, but much experimentation to reach optimal constants is surely undesirable.

In order to understand why the Ogden material model has difficulties in fitting these assumed data, we examine $w'(e)$ corresponding to $\tau(e)$ from Equation (7). In this case,

$$w'(e) = w'_{nh}(e) + w'_p(e) \tag{10}$$

where $w'_{nh}(e)$ corresponds to $\tau_{nh}(e)$ and $w'_p(e)$ corresponds to $\tau_p(e)$. Clearly $w'_{nh}(e) = \exp(2e) - 1$. Figure 5 shows $w'_p(e)$, $w'_p(-\frac{1}{2}e)$, and $w'_p(e) - w'_p(-\frac{1}{2}e)$, from the exact solution (Equation (5)) and from the Ogden fit. We see that $w'_p(e)$ is an oscillating function of $e$, and, in general, oscillating functions are not well fit by series of exponentials.

We use 46 uniform splines for the representation of $w'(e)$, and the relative error $r$ in Equation (6) is less than 1%. Hence, the lines representing the test data and our model in Figure 5 are practically identical.

### *4.2. Wavy stress–strain test data*

Assume that the test data are given by the following function, in the strain range $-2 \leqslant e \leqslant 2$:

$$\tau(e) = w'(e) - w'(-\tfrac{1}{2}e), \quad w'(e) = (\exp(3e) - \exp(-3e))(1 + 0.2\sin(10e)) \tag{11}$$

where $\tau(e)$ is plotted in Figure 6.

In this case, the Ogden material model with $\alpha_n = n, n = 1, \ldots, 9$, produces a wildly oscillating fit in which the small-strain Young's modulus is negative. A better Ogden material model fit is obtained with the three terms $(\mu_1 = 0.519, \alpha_1 = 1.3)$, $(\mu_2 = 0.023, \alpha_2 = 5.0)$, and $(\mu_3 = -6.510, \alpha_3 = -2.0)$. However, although this fit follows the trend of the test data well, it does not follow the waves in the data. Also, this fit does not follow the small-strain behavior of the test data. As in the first example, the series of exponentials associated with the Ogden model cannot easily fit the oscillations in $w'(e)$.

In our representation of the response, we use 42 uniform splines for the fit, and the relative error $r$ in Equation (6) is less than 1%. Therefore, the lines given in Figure 6 for the test data and our model are indistinguishable.

## 5. CONCLUSIONS

The objective in this paper was to present a material model for incompressible isotropic hyperelastic material behavior. The distinguishing features of the model are that it is based on a strain energy description separable in terms of logarithmic strains, a piecewise spline representation of measured uniaxial tension–compression test data, and a piecewise spline representation of the strain energy density.

The restrictions of the model are hence that the separable strain energy description must be applicable and that the test data, obtained over a sufficient range of strain, should represent the general material behavior. In particular, test data must be available for both tension and compression. The model is attractive because it is easy to use and represents, in the description of the test data, a generalization of the Ogden model. It replicates the test data very accurately, for small and large strains, and for tension and compression, even if these data represent a complex behavior.



DOI: 10.1002/cnm

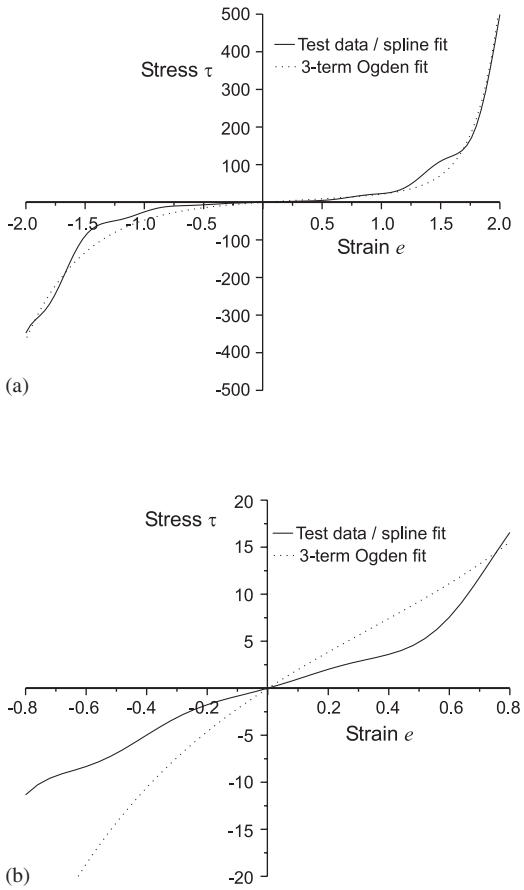


Figure 6. Original data and curve fits for wavy data: (a) full range of strains and (b) enlargement near the origin.

However, although our model is powerful in representing complex and wavy behavior, it is obviously important to make sure that experimental errors (corresponding to non-physical wavy material behavior) have been removed from the data points before applying the model. We anticipate that if the data points correspond to a stable material, then our approach will produce a stable material description, and if the data points correspond to an unstable material, then our approach will produce an unstable material description.

The capability of representing complex test data accurately may also mean that the model may be useful in directly describing new materials of hyperelasticity, but this aspect needs of course further study.

The material model is well suited for implementation in finite element analysis. In plane stress conditions, the model can be directly used with displacement-based finite elements. In axisymmetric, plane strain, and 3-D conditions, the model can be modified to be 'slightly compressible', and then displacement–pressure elements can be used to avoid locking [1, 11]. The implementation effort is similar to the implementation effort required for the Ogden model.



DOI: 10.1002/cnm

## REFERENCES


1. Bathe KJ. *Finite Element Procedures*. Prentice-Hall: Englewood Cliffs, NJ, 1996.
2. Boyce MC, Arruda EM. Constitutive models of rubber elasticity: a review. *Rubber Chemistry and Technology* 2000; **73**(3):504–523.
3. van den Bogert PAJ, de Borst R. On the behaviour of rubber-like materials in compression and shear. *Archive of Applied Mechanics* 1994; **64**:136–146.
4. Mooney M. A theory of large elastic deformation. *Journal of Applied Physics* 1940; **2**:582–592.
5. Carmichael AJ, Holdaway HW. Phenomenological elastomechanical behavior of rubbers over wide ranges of strain. *Journal of Applied Physics* 1961; **32**(2):159–166.
6. Valanis KC, Landel RF. The strain-energy function of a hyperelastic material in terms of the extension ratios. *Journal of Applied Physics* 1967; **38**(7):2997–3002.
7. Kearsley EA, Zapas LJ. Some methods of measurement of an elastic strain-energy function of the Valanis–Landel type. *Journal of Rheology* 1980; **24**(4):483–500.
8. Ogden RW. *Non-Linear Elastic Deformations*. Ellis Horwood: Chichester, U.K., 1984.
9. Jones DF, Treloar LRG. The properties of rubber in pure homogeneous strain. *Journal of Physics D*: *Applied Physics* 1975; **8**:1285–1304.
10. Hamming RW. *Numerical Methods for Scientists and Engineers*. Dover: New York, 1973.
11. Sussman T, Bathe KJ. A finite element formulation for nonlinear incompressible elastic and inelastic analysis. *Journal of Computers and Structures* 1987; **26**:357–409.




DOI: 10.1002/cnm